



Article

Traffic and Industrial Contributions of Particle-Bound PAHs during an Air Pollution Event in the Metropolitan Area of Medellin-Colombia: Inhalation Intake Risk during Pregnancy

Jhon Fredy Narváez-Valderrama ^{1,*}, Sandra Viviana Alzate-B ¹, Vanessa Correa-Gil ², Juan José García-L ¹, Juan Mauricio Bedoya-Soto ¹, Francisco José Molina-P ³, Gladys Guillermrina Pauta-Calle ⁴, Gabriela Belén Vázquez-Guillén ⁴ and Carlos D. Ramos-Contreras ³

¹ Grupo de Investigación Ingenier, Facultad de Ingeniería, Corporación Universitaria Remington, Calle 51 No. 51-27, Medellín 050010, Colombia; sandra.alzate.9669@miremington.edu.co (S.V.A.-B.); juan.garcia.3750@miremington.edu.co (J.J.G.-L.); juan.bedoya@uniremington.edu.co (J.M.B.-S.)

² Grupo de Investigaciones Biomédicas UniRemington, Corporación Universitaria Remington, Calle 51 No. 51-27, Medellín 050010, Colombia; dr.vacogi@gmail.com

³ Grupo de Investigación en Gestión y Modelación Ambiental—GAIA, Facultad de Ingeniería, Universidad de Antioquia U.de.A, Calle 70 # 52-21, Medellín 050010, Colombia; francisco.molina@udea.edu.co (F.J.M.-P.); daniel.ramos@udea.edu.co (C.D.R.-C.)

⁴ Laboratorio de Sanitaria de la Facultad de Ingeniería de la Universidad de Cuenca, Cuenca 10107, Ecuador; guillermrina.pauta@ucuenca.edu.ec (G.G.P.-C.); gabriela.vazquez@ucuenca.edu.ec (G.B.V.-G.)

* Correspondence: jhon.narvaez@uniremington.edu.co



Citation: Narváez-Valderrama, J.F.; Alzate-B, S.V.; Correa-Gil, V.; García-L, J.J.; Bedoya-Soto, J.M.; Molina-P, F.J.; Pauta-Calle, G.G.; Vázquez-Guillén, G.B.; Ramos-Contreras, C.D. Traffic and Industrial Contributions of Particle-Bound PAHs during an Air Pollution Event in the Metropolitan Area of Medellin-Colombia: Inhalation Intake Risk during Pregnancy. *Atmosphere* **2024**, *15*, 173. <https://doi.org/10.3390/atmos15020173>

Academic Editor: Kai-Jen Chuang

Received: 7 September 2023

Revised: 14 November 2023

Accepted: 20 November 2023

Published: 30 January 2024



Copyright: © 2024 by the authors. Licensee MDPI, Basel, Switzerland. This article is an open access article distributed under the terms and conditions of the Creative Commons Attribution (CC BY) license (<https://creativecommons.org/licenses/by/4.0/>).

1. Introduction

Particulate matter (PM) is produced by natural and human activities which pollute the air [1,2]. Depending on its source, PM may include a diverse range of polycyclic aromatic hydrocarbons (PAHs), which induce health problems, including endocrine disorders in vulnerable populations, such as those of older adults, children, and pregnant women [3]. PAHs primarily emanate from sources such as fuel fossil combustion, forest fires, and industrial emissions, posing a potential risk due to chronic exposure. For instance, in

eastern China, PAH concentrations are mainly produced by industrial and traffic emissions, presenting seemingly negligible cancer risks for adults but significantly heightened risks for children. Additionally, residing within 50 m of a high-traffic road has been significantly linked to spontaneous abortion (SAB) [4]. Thus, the screening of PAH levels for public health studies should prioritize industrial and traffic emissions.

The impact of PAHs is particularly high in pregnant women because the physiological changes in their bodies may increase the intake of air by 10%, leading to a similar elevation of PAHs in the lungs [5,6]. As many airborne pollutants are in maternal blood, PAHs have the potential to diffuse into the fetal environment through the placenta–blood interchange [7,8]. Specifically, high concentrations of PAHs were found by E. Drwal and coworkers in maternal blood, including the carcinogenic congener benzo[a] pyrene (BaP), at concentrations of $0.75 \text{ ng} \times \text{mL}^{-1}$ [9]. Although PAHs decrease their concentration four times upon crossing the placenta, this reduction does not prevent their impact on the intrauterine growth restriction (IUGR) [10]. Also, researchers have reported risk values associated with exposure to BaP and c-PAHs. Thereby, human exposure to approximately $1.6 \text{ ng} \times \text{m}^{-3}$ of BaP or $10 \text{ ng} \times \text{m}^{-3}$ of c-PAHs, including BaP, BaA, Bb + kF, BghiP, CHRY, DahA and IND, has been linked to increased DNA adducts and decreased repair efficiency [11]. These c-PAHs (5–7 rings and molecular weight between 252 and $300 \text{ g} \times \text{mol}^{-1}$) are associated with breathable PM2.5. Therefore, congeners such as BaP, CHRY, IND, and DahA, among others, may be found in the blood, placenta, and maternal–fetal cord white blood cells in pregnant women exposed to air pollution [12,13]. For instance, in case studies, BaP has been found at higher levels in the placentas of a preterm delivery group compared to those of a full-term delivery group [14].

Air pollution increases pregnancy disorders such as the higher miscarriage rate observed in most pollutant cities [15]. In developed countries, pregnancy outcomes and maternal care are relevant, and missed abortion is a worldwide concern. However, missed abortion etiology is a multifactorial issue in which air pollution plays a key role [15]. Also, a significant relationship between c-PAH levels and a decreasing concentration of redox biomarkers provides an indication of the oxidative stress pathways associated with preterm labor [13].

Located in the northwestern corner of tropical South America, the Metropolitan Area of Medellin-Colombia (MAMC) is situated in the mountains of the Colombian Andes within a narrow and deep valley with elevations ranging between 1400 and 2400 masl. This valley has a maximum width of 17 km and an average length of 45 km, and its main river flows predominantly from south to north. Also, the MAMC experiences prevailing, low-level, north-to-south atmospheric winds [16], which are influenced by the northeast trade winds that dominate the region's climatology [17]. This wind pattern implies greater rainfall over the southern MAMC compared to the northern [16]. The missed abortion rate in the MAMC has recently increased, but the effect of air pollution on this tendency remains unknown. Despite a decline in air quality over the past years, placing the MAMC among the regions with the poorest air quality in Latin America [18], crucial information regarding the primary sources and locations with a heightened risk (hazardous places for pregnancy exposure) of airborne PAHs is still elusive. Also, the associations between the PAH impact, the sources, and the meteorological factors have not been carried out in the MAMC.

This paper introduces a real-time tracking analysis conducted in the MAMC, employing both individual airborne PAHs and total congeners assessed by GC/MS, alongside real-time monitoring. This real-time analysis was conducted to estimate exposure levels in residential places influenced by traffic and industrial emissions and to offer insights into the varying risks faced by individuals living under these conditions. Our aim was to establish a preliminary association between the missed abortion rate and air quality in the MAMC. The monitoring period spanned from September to October 2021, a critical season for PM2.5 in the MAMC (see Figure 1b). This focused timeframe ensures the relevance of the second peak of the bimodal tendency for PM2.5 emissions in the region.

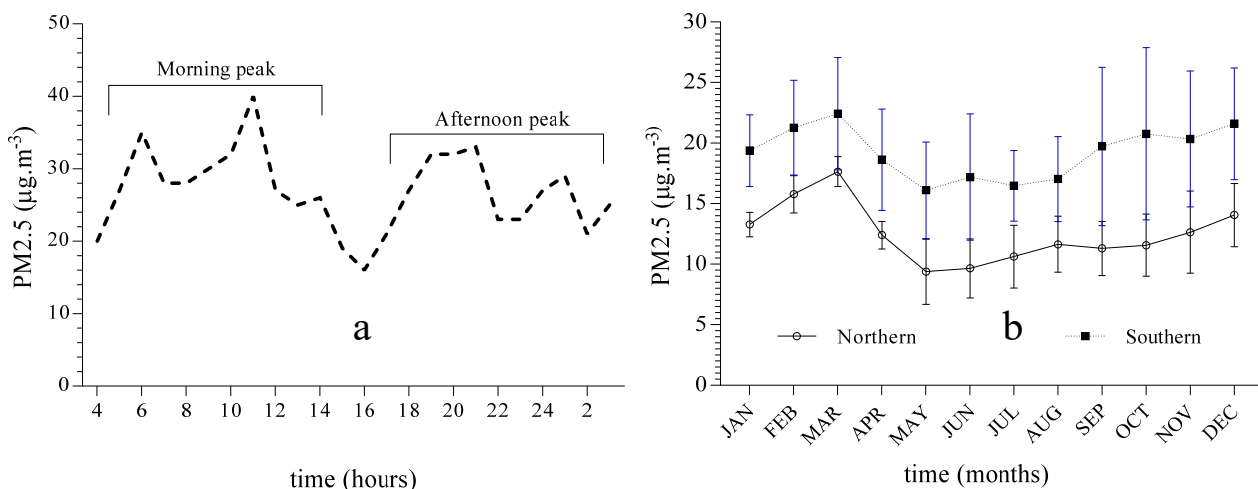


Figure 1. Typical tendency for concentration of PM2.5 in MAMC for 2021. (a) Diurnal concentration of PM2.5. (b) Annual cycle of PM2.5 concentration. A bimodal tendency is shown by both cycles.

2. Materials and Methods

2.1. Study Area and Air Pollution Event during 2021

For the real-time monitoring of PAHs, three distinct locations were selected in both the northern and the southern regions of the MAMC. The photoelectric sensor was deployed exclusively in residential places (RES), residential areas influenced by traffic contribution (RES + TRAF), and those residential areas affected by industrial sources (RES + IND). In contrast, fixed air quality gauges were employed for PAHs analysis via GC/MS in both the northern and southern MAMC. Refer to Figure 2. Additionally, recognizing the potential influence of the distance between air pollution sources and pregnant women on adverse perinatal outcomes, we strategically positioned our monitoring equipment. For exclusively residential areas, we placed the monitoring equipment at a minimum distance of 50 m from the emission sources, including vehicles and industrial emissions [4]. Conversely, the residential places influenced by traffic and industrial activity were located at a distance of less than 50 m from the emission sources (see Figure 2c,d).

2.2. Chemical and Reagents

The stock solution of PAH congeners (16 priority tests), 7 deuterated PAHs (quantification purposes), and the stock solution of 16 individual PAHs were purchased from sigma Aldrich (Purity > 99.5%). Similarly, the organic solvents such as hexane and methanol, employed for extracting and preparing the stock solution of PAHs, were purchased from sigma Aldrich (Gas chromatography MS SupraSolv[®], Darmstadt, Germany). Finally, the capillary column (30 m, 0.25 mm, and 0.15 μm) was supplied by Restek Pure Chromatography.

2.3. Airborne PAH Analysis by GC/MS

Quartz filters for the particle-bound PAH analysis were supplied by the MAMC, which oversees the air quality monitoring network. These filters were taken out of high flow samplers (average flow of $1.13 \text{ m}^3 \times \text{min}^{-1}$ for 24 h) deployed in representative locations in both the southern and northern regions for PM2.5 collection. The sampled filters were kept at -20°C . Therefore, the filters were cut into small circular pieces (16 mm diameter) and subjected to extraction using pressurized hot water extraction (PHWE) using a Thermo Scientific[®] Dionex[®] ASE[®] 350 system (Thermo Fisher Scientific, Sunnyvale, CA USA). The extraction process employed a 90:10 ratio of water to methanol at 200°C and 2000 psi, with a single extraction cycle.

The aqueous extract underwent liquid–liquid micro-extraction with ultrapure hexane (Merck[®], Darmstadt, Germany). The PAHs from the organic phase were identified by a Thermo Scientific Trace[®] Ultra coupled to a mass spectrometry detector (ISQ) in the

mode of selected ion monitoring (SIM) under electronic impact (70 eV). The separation of PAH congeners occurred on a select PAH capillary column (30 m, 0.25 mm (about 0.01 in), 0.15 μm) with initial and final temperatures of 70 °C and 320 °C, respectively. Helium served as the carrier gas (2 mL \times min $^{-1}$). Quantification was accomplished using seven deuterated internal standards (ISTD) [19].

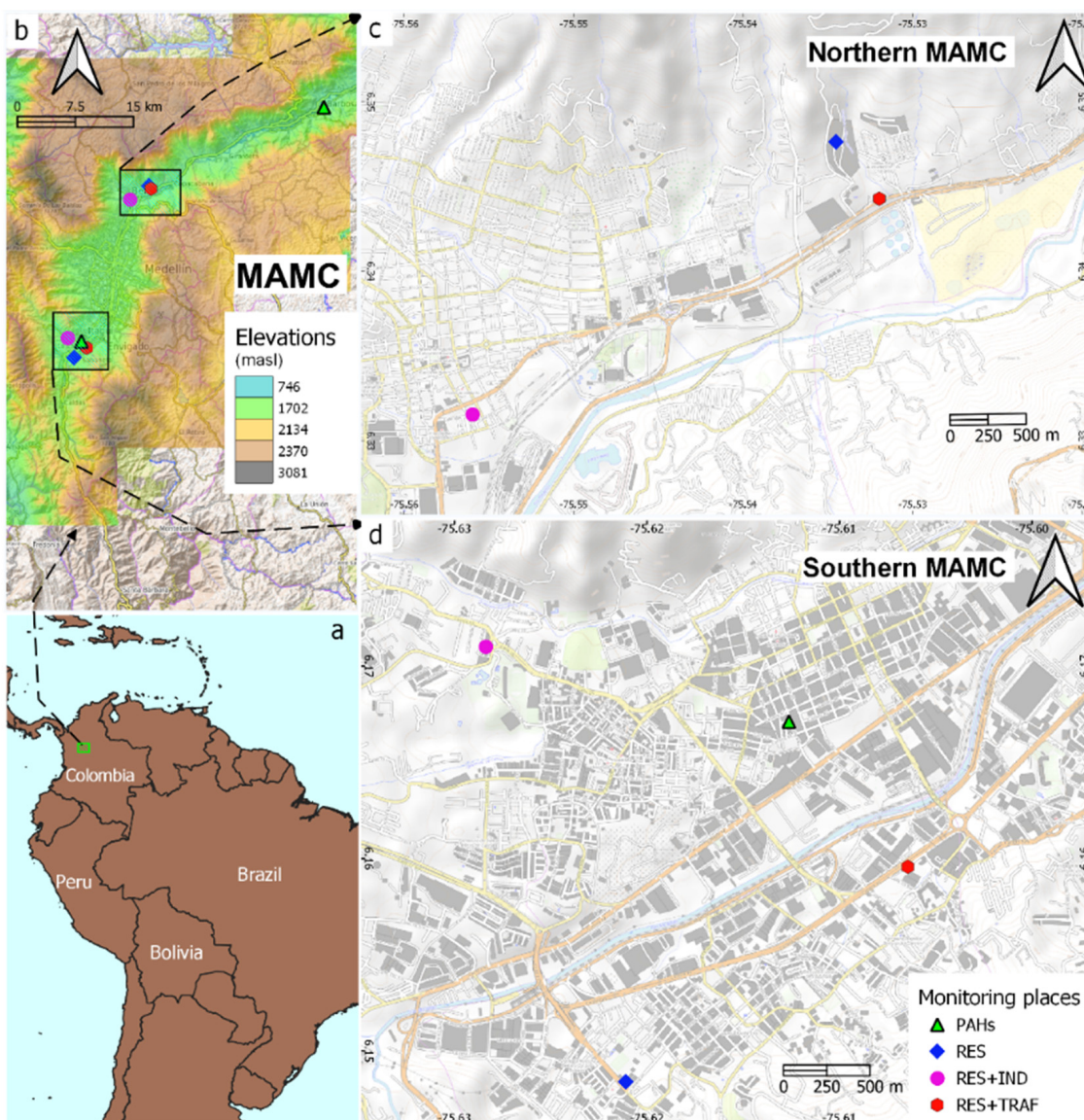


Figure 2. (a) General location of the MAMC in northwestern tropical South America. (b) The MAMC is placed in an inter-Andean and narrow valley. (c) Monitoring places for PAH analysis in northern MAMC. (d) Monitoring places for PAH analysis in southern MAMC. Blue: exclusively residential places (RES); red: residential places influenced by traffic vehicles (RES + TRAF); purple: residential places influenced by industrial activities (RES + IND).

2.4. PAH Emission Sources

The emission sources in the southern and northern regions of the MAMC were assayed according to the ratios between the concentrations of fluoranthene (FLU) and pyrene (PYR) and plotted on the y-axis against the ratios between the concentration of benzo[a]anthracene (BaA) and the sum of BaA and chrysene (CHR) on the x-axis. This analysis was based on a previously established methodology to estimate PAH sources such as petrogenic, coal combustion, and vehicular emissions (petrol or diesel) [20].

2.5. Real-Time Monitoring of Total PAHs (Exposure Levels)

The real-time PAH analysis was conducted between September and November 2021 in both the southern and northern regions of the MAMC. This timeframe coincides with the second peak of the bimodal tendency for PM2.5 emissions in the MAMC (see Figure 1b). Considering the geomorphological features and the predominant north-to-south wind direction in the MAMC, the monitoring places were strategically selected in the northern and southern regions (see Figure 2c,d). The total airborne PAH levels were monitored using the photoelectric sensor PAS 2000 (EcoChem Analytics, League City, TX, USA) with a UV radiation detector. The quantification range for the analytical method was from 0 to $4000 \text{ ng} \times \text{m}^{-3}$, with a lower threshold of $10 \text{ ng} \times \text{m}^{-3}$. The flow rate was $5 \text{ L} \times \text{min}^{-1}$, which is similar to that of minute ventilation during breathing in pregnancy, and the device was deployed in each monitoring place for 24 h. The real-time data were collected using the PAHDAS software, outputting txt file, and were subsequently processed in Microsoft Excel format (2016—v16.0) and the R Project for Statistical Computing®.

2.6. Risk Assessment by Inhalation Intake for Pregnant Women

The risk of long-term inhalation exposure for pregnant women was assessed using the inhalation intake model (I_a) [21]. See Equation (1):

$$I_a = \frac{C_a \times IR_a \times t_{Ea} \times f_E \times ED}{BW \times T_{ave}} \quad (1)$$

where C_a is the contaminant concentration in air ($\text{mg} \times \text{m}^{-3}$), IR_a is the inhalation rate ($\text{m}^3 \times \text{h}^{-1}$), t_{Ea} is the time dependent on the duration of exposure ($\text{h} \times \text{day}^{-1}$), f_E is the exposure frequency ($\text{day} \times \text{year}^{-1}$), ED is the exposure duration (years), BW is body weight (kg), and T_{ave} is the average period of exposure (day). The I_a model was applied for the exposure in both the southern and northern regions of the MAMC, which allowed the assessment of the maximum pregnancy risk exposure in the city. The body weight parameter was defined based on the average weight of a woman in the MAMC (65 kg) plus the recommended weight gain during pregnancy according to the World Health Organization (WHO) guidelines (12 kg).

2.7. Correlation between Missed Abortion Rate and Averaged Levels of PM2.5 as an Indicator of PAHs in the MAMC

The missed abortion rate data were extracted from the harmonized databases of Dirección Seccional de Salud de Antioquia (DSSA—<https://dssa.gov.co/index.php/vigilancia-en-salud-publica>). Accessed on 20 march 2020. This comprehensive database, serving both the northern and southern regions of the MAMC, includes only missed abortion (miscarriage and stillbirth) and operates as a unified dataset. In this research, the missed abortion rate in the MAMC was analyzed by applying a Student's *t*-test to find the significant differences ($p < 0.05$) of missed abortion between the northern and southern regions of MAMC.

A correlation between PM2.5 and the total PAHs was estimated through real-time analysis of both parameters simultaneously. The PAH levels were analyzed by the photoelectric sensor PAS 2000 (refer to Section 2.5), while the PM2.5 was analyzed using the continuous particle analyzer PM2.5 BAM-1020 (Met One instruments, Inc., Grants Pass, OR, USA). Both instruments were connected to a datalogger and to monitoring system georeferencing capabilities. Furthermore, the annual variation data for PM2.5 were obtained from Sistema de Alertas Tempranas del Valle del Aburrá (SIATA—https://siata.gov.co/siata_nuevo/) accessed on 20 March 2020).

The data for missed abortion and PM2.5 spanned the period from 2012 to 2020, focusing on pregnant women aged 25–34 years in both the northern and southern regions of the MAMC, irrespective of their specific residential locations when experiencing missed abortion. The data were graphed for descriptive statistical analysis, tendencies, and differences

in the missed abortion rate between the south and the north by a Pearson correlation for tendencies study.

2.8. Diurnal Cycle of Winds and Air Temperature in the MAMC

To investigate the impact of meteorological factors on PAH concentrations in the MAMC domain, we used hourly data obtained from the ERA-5 reanalysis downscaled at 12.5 km within the spatial domain of 5.75 N–6.75 N/76 W–75 W (<https://cds.climate.copernicus.eu/cdsapp#!/home> accessed on 10 July 2023). Our focus centered on estimating the diurnal cycles (i.e., the averaged values at a sub-daily timescale) of the wind velocity and temperature at low-pressure levels (825–875 hPa) over the MAMC. Specifically, we conducted a detailed analysis and visualization of the wind vectors along with the temperature fields for the months of September, October, and November 2021. These months are pertinent to the event under investigation, which encompasses both total PAHs and individual analyses by GC/MS.

2.9. Data Analysis

The data were plotted using the GraphPAD Prism 7.0 and R project. The differences in the missed abortion rates between both the southern and northern regions were assessed using a Pearson correlation (confidence interval >95%). Finally, real-time PAH data were processed in Microsoft Excel format (2016—v16.0) and the R Project.

3. Results

3.1. Analysis of Airborne PAHs (Exposure Levels)

The select PAH capillary column effectively separated all the PAH congeners, with identification based on the target ions outlined in Table 1. Overall, the validation data demonstrated acceptable values for the quantification of particle-bound PAH through GC/MS analysis and PHWE. Notably, PHWE showed a robust recovery method (>60%) using spiked deuterated surrogates. The limits of detection (LOD) and quantification (LOQ), as well as the linearity, were significant for our quantification purposes (see Table 1). Additionally, the assessments of the homoscedasticity and even the $r^2 = 0.99$ indicated a good linearity. See Table 1.

Table 1. Chromatography parameters and validation. The quantification method was carried out by deuterated internal standard (ISTD)-ACP-d10, CHRY-d12, NAP d8, Perylene-d12, and PHE-d12.

PAH Congeners	Rings	Molecular Weight (g × mol ⁻¹)	tR (Min)	Target Ion	LOD ($\mu\text{g} \times \text{L}^{-1}$)	LOQ	Range ($\mu\text{g} \times \text{L}^{-1}$)	r^2
Naphthalene (NAP)	2	128.17	3.30	128	6.1	18.4	3–300	0.996
Acenaphthylene (ACPY)	3	152.19	4.79	152	2.9	10.0	3–300	0.995
Acenaphthene (ACP)	3	154.21	4.95	153	7.0	22.0	3–300	0.997
Fluorene (FL)	3	166.22	5.77	166	30.8	90.0	3–300	0.995
Phenanthrene (PHE)	3	178.23	8.37	178	4.0	12.0	3–300	0.991
Anthracene (ANT)	3	178.23	8.50	178	16.5	50.0	3–300	0.999
Retene (RET)	3	234.34	13.25	202	15.0	45.1	3–300	0.995
Fluoranthene (FLU)	4	202.26	12.82	202	15.0	45.1	3–300	0.994
Pyrene (PYR)	4	202.26	13.99	202	10.0	30.0	3–300	0.997
Benz[a]anthracene (BaA)	4	228.29	19.52	228	16.5	50.0	3–300	0.998
Chrysene (CHRY)	4	228.28	19.88	228	33.0	100.0	3–300	0.999
Benzo[b,f] fluoranthene (BbF)	5	252.31	24.62	252	22.3	67.0	3–300	0.993
Benzo[k]fluoranthene (BkF)	5	252.31	24.72	252	20.0	60.3	3–300	0.997
Benzo[a]pyrene (BaP)	5	252.31	26.37	252	33.0	100	3–300	0.996
Dibenz[a,h]anthracene (DahA)	5	278.35	31.74	278	60.8	180.0	3–300	0.996
Indeno[1,2,3-cd] pyrene (IND)	6	276.33	31.73	276	23.7	71.0	3–300	0.996
Benzo[ghi]perylene (BghiP)	6	276.33	33.65	276	23.7	71.0	3–300	0.999

Low levels of light PAHs were found in both the northern and southern regions; in contrast, the heavier PAHs showed higher amounts (see Figure 3). Individual PAHs were detected in the PM from the MAMC, revealing significant differences between the northern and southern regions with regard to the total PAH congeners. Additionally, the spatial differences in the levels of heavy PAHs were notable. In particular, the total concentration of individual PAH congeners showed a concentration of $5.3 \text{ ng} \times \text{m}^{-3}$ in the northern MAMC and $16.82 \text{ ng} \times \text{m}^{-3}$ in the southern MAMC, indicating that the southern region experienced PAH levels 3.2 times higher than the northern ones (see Figure 3). Similarly, the total levels of heavy PAHs in the northern region were measured at $1.33 \text{ ng} \times \text{m}^{-3}$, while the southern region showed markedly higher levels of $12.39 \text{ ng} \times \text{m}^{-3}$. Heavy PAHs are widely studied because of their carcinogenic potential effect (c-PAHs). The main c-PAH congener, BaP, showed levels of $0.35 \text{ ng} \times \text{m}^{-3}$ in the southern regions, while in the northern region they were $0.07 \text{ ng} \times \text{m}^{-3}$ (see Figure 3).

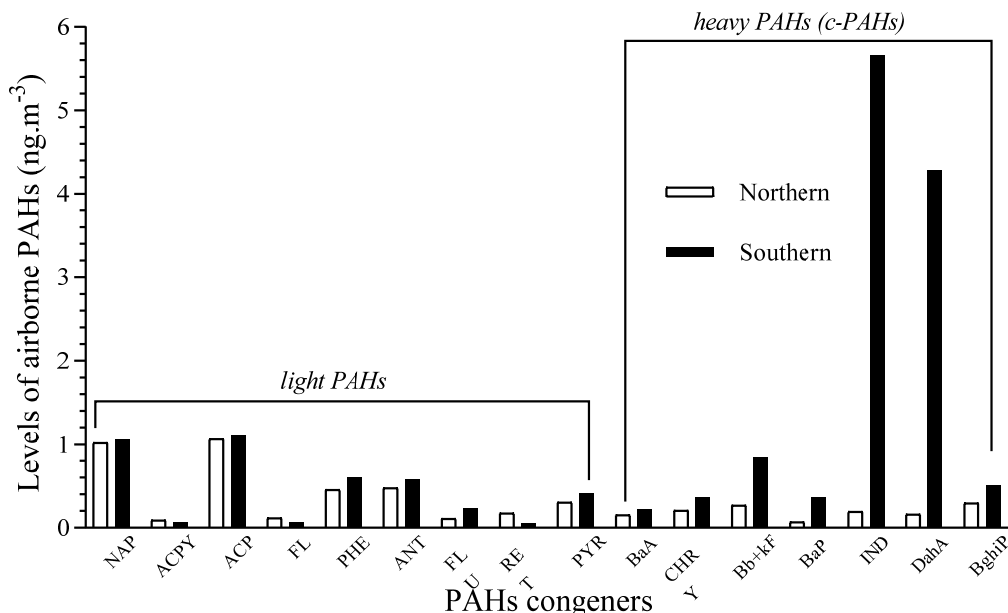


Figure 3. Averaged levels of airborne PAHs in southern and northern locations in Medellin city ($n = 66$).

The analysis of PAH emission sources, particularly vehicular emissions, highlighted vehicular combustion as the predominant contributor to the levels of PAH congeners, as illustrated in Figure 4. The pollution emission sources in the MAMC were identified through diagnostic ratios between the PAH congeners [20,22]. This analysis, depicted in Figure 4, underscores vehicular emissions, both diesel and petrol, as significant contributors to airborne PAHs. Specifically, our results emphasize petrol emissions as the primary source. Consequently, residential areas influenced by traffic (RES + TRAF) may be regarded as presenting a higher risk.

In the southern MAMC, the levels of BaP were lower than the established risk value associated with DNA repair disruption (Table 2). However, the c-PAH levels exceeded the thresholds, potentially impacting DNA repair as a marker for genetic damage. See Table 2 for reference values. In contrast, in the northern MAMC, the concentrations of BaP and c-PAHs did not exceed the established risk values for exposure. The identified differences between the northern and southern regions underscore the need for further studies to comprehensively assess the risk of the genetic implications and potential health issues associated with airborne PAH exposure in the southern MAMC.

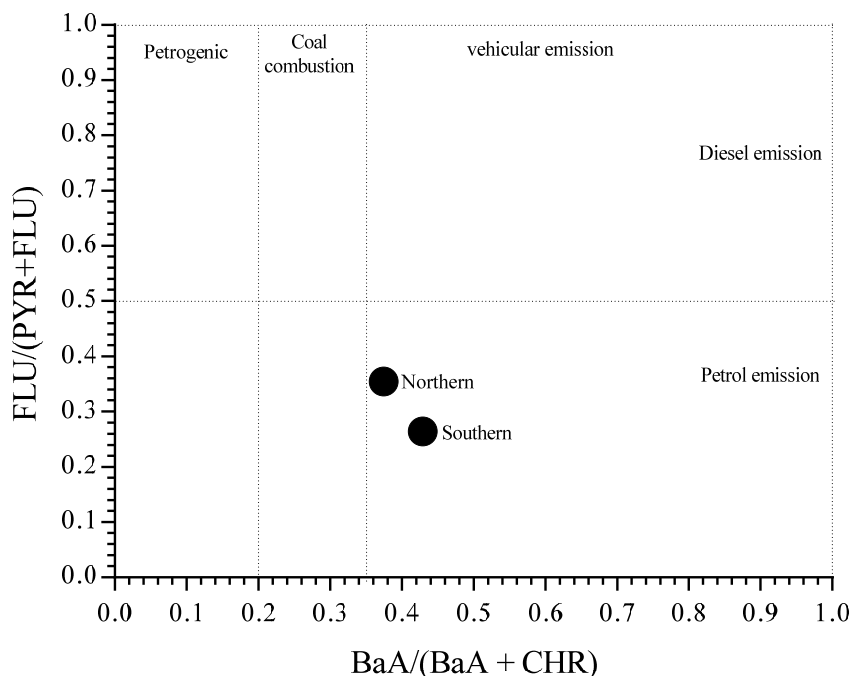


Figure 4. Ratios between individual congeners and their main sources of air pollution. Both PAH levels (northern and southern) were shown to be from petrol emissions.

Table 2. Thresholds values for DNA damage by DNA adducts due to PAH exposure [19].

	Northern ($\text{ng} \times \text{m}^{-3}$)	Southern ($\text{ng} \times \text{m}^{-3}$)	Values May Affect DNA Repair by DNA Adducts ($\text{ng} \times \text{m}^{-3}$)
Value of BaP	0.07	0.372	1.6
Value of c-PAHs	1.48	12.39	10

3.2. Real-Time PAH Monitoring

During the air pollution event analyzed in the MAMC, the exposure levels of PAHs showed a diurnal variation in both the northern and southern regions of the MAMC (see Figure 5). In general, higher concentrations of PAHs were observed in the RES + IND and RES + TRAF places compared to purely residential areas (RES). This pattern reveals the contribution of these substances by anthropogenic activities. Figure 5 specifically illustrates that the RES + TRAF and RES + IND monitoring places show higher levels of total airborne PAHs compared to the RES places, displaying a bimodal behavior with morning and afternoon peaks. Further real-time analysis of the airborne PAHs revealed that during rush hours, the total PAH concentrations in the RES places exceeded $50 \text{ ng} \times \text{m}^{-3}$, while the RES + TRAF and RES + IND places reached values three times higher ($>150 \text{ ng} \times \text{m}^{-3}$) (see Figure 5). Similarly, the total airborne PAHs in the southern region were slightly higher compared to those of the northern MAMC. Approximately, the diurnal cycle of PAH levels peaks between 06:00 and 10:00 LST (morning peak) and 16:00 and 20:00 LST (afternoon peak). The afternoon peak aligns with the rush hour and reflects the average diurnal patterns of air pollution in the MAMC [23].

The diurnal concentration of PM2.5 (Figure 1a) and the annual cycle of PM2.5 concentration (Figure 1b) revealed a bimodal tendency and depicted the typical patterns of PM2.5 levels in the MAMC at diurnal and annual timescales. The diurnal PAH analysis in Figure 5 also showed a similar trend.

Using ERA-5 hourly data, Figure 6 depicts the diurnal wind and temperature cycle at 825–875 hPa, averaged for September–October–November (SON) of 2021. From 8 pm to 8 am, as the temperature decreases in the MAMC, the atmospheric wind flows from the north to the south (see Figure 6). As the temperature increases between 8 am and 2 pm,

easterly and southeasterly winds dominate, enabling the transport of aerosols. Finally, from 2 pm to 8 pm (Figure 6), when the temperature reaches its maximum values, easterly winds prevail, but a southerly wind component emerges in the northern MAMC.

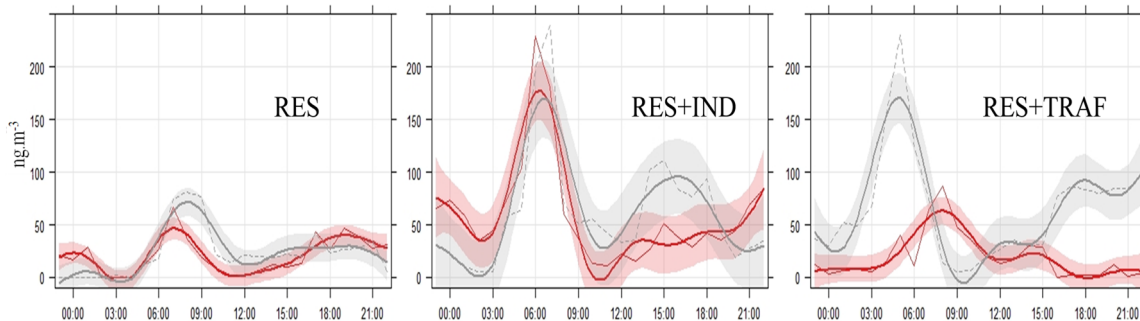


Figure 5. Analysis of diurnal patterns of airborne PAHs by real-time analyzer for 24 h for different monitoring places. Red line: northern MAMC; gray line: southern MAMC.

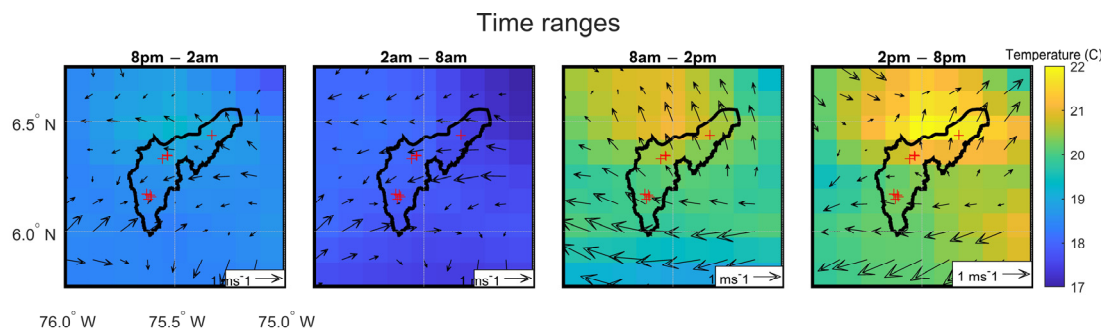


Figure 6. Diurnal cycle of wind and air temperature at 825–875 hPa, averaged for September–October–November (SON) 2021. Black line represents the MAMC borders. Monitoring places are shown as red crosses.

Due to minimum temperatures in the early morning (Figure 6, 2 am–8 am), a larger stable layer forms in the southern MAMC. After 8 am, as temperatures rise, the aerosols are resuspended to higher elevations in the southern MAMC. The resuspended aerosols remain during the morning until the onset of easterly winds. Thus, if the elevated aerosols reach the mountain tops, the aerosols may be depurated. In contrast, if the aerosols remain below the tops of the mountains, they are re-transported to the north when the wind shifts in that direction (2 pm–8 pm, Figure 6). After 8 pm, as the temperature drops and the northeasterly winds prevail, the aerosols are deposited again, reaching higher levels, and forming a stable layer in the southern MAMC (Figure 6). Similarly, a small stable layer is formed in the northern MAMC, but the temperature gradients and wind direction move the aerosols southward, allowing some amounts to be depurated by the winds because the northern temperatures are higher, leading to higher elevations of aerosols and their depuration to the west.

3.3. Inhalation Intake Risk Assessment for Pregnant Women

The inhalation intake risk model showed elevated values in the southern MAMC compared to the northern MAMC, with the highest risk observed in RES + TRAF and RES + IND. The risk assessment for the comparison of the pregnancy exposure to PAHs between the northern MAMC and the southern MAMC is presented in Table 3. The I_a value was estimated by applying Equation (1). In the southern MAMC, the inhalation intake in RES + TRAF and RES + IND was three times higher than in RES (see Table 3). Additionally, the total of the airborne PAHs in the southern MAMC was 3.2 times higher than in the northern region (see Figure 2). Consistently, the data on the missed abortion rates in the MAMC

reveal a twofold higher ratio in the south compared to the north [23]. This fact suggests a potential relationship between vehicular and industrial emissions and increased exposure during pregnancy.

Table 3. Risk assessment for airborne PAHs (I_a).

Monitoring Place	Location	I_a ($\mu\text{g} \times (\text{kg} \times \text{day})^{-1}$)
RES	Northern	0.10
RES + TRAF		0.09
RES + IND		0.28
RES	Southern	0.11
RES + TRAF		0.31
RES + IND		0.29

Rochelle and coworkers showed significant associations between living within a distance of 50 m from a high-traffic road and spontaneous abortion (SAB) [4]. Additionally, Perera et al. found that airborne PAHs may be associated with miscarriage mechanisms because some congeners were bound to DNA (PAH–DNA adducts) in maternal–fetal cord white blood cells [11]. Therefore, the association between SAB and airborne PAH exposure should be considered in the risk assessments for pregnant woman.

Low levels of RET congener in the MAMC indicate that forest fires are not the principal source of PAH emission. For more details, see Figures 2 and 3. In fact, the predominant sources of airborne PAHs detected around RES areas are associated with fuel burning from traffic and industries [24]. Vehicular emissions, specifically those from petrol fuel, emerge as the main source for airborne PAHs in the MAMC (see Figure 3), and, as previously presented, the heavier congeners, such as Bb + kF, BeP, BaP, IND, DahA, and BghiP (c-PAHs), showed the highest differences between the northern and southern regions in the MAMC. These congeners are typically detected in PM2.5 and PM10 due to their greater lipophilic properties related to the IUGR at levels exceeding $40 \mu\text{g} \times \text{m}^{-3}$ through exposure in the first gestational month [25].

3.4. Implication of Air Pollution Exposure on Pregnancy in the MAMC

Globally, PAHs are recognized as key air pollutants impacting pregnancy outcomes and are often associated with PM2.5. The missed abortion rate in the southern MAMC during 2005–2020 was 1.4 times higher than in the northern MAMC (see Figure 7).

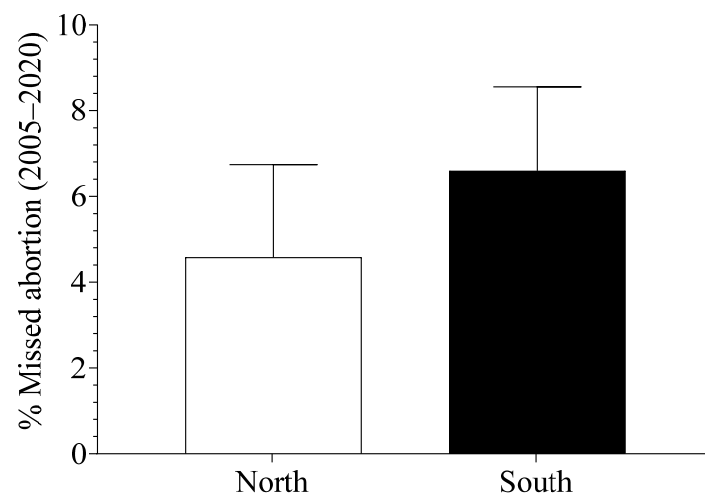


Figure 7. Differences in the percentages of missed abortion between northern and southern regions in the MAMC (2005–2020).

While the annual data for total PAHs in recent years may be unavailable in the MAMC, the PM2.5 data are accessible. Through continuous monitoring of the northern to the southern MAMC regions (see Figure 8a,b), the significant correlation estimated between PAHs and PM2.5 ($r = 0.69$, $p < 1\%$ in Figure 3b) highlights their unequivocal association in this region [26]. The relation of PM2.5–PAHs is also influenced by the effects of meteorological conditions and/or source emission variability [26].

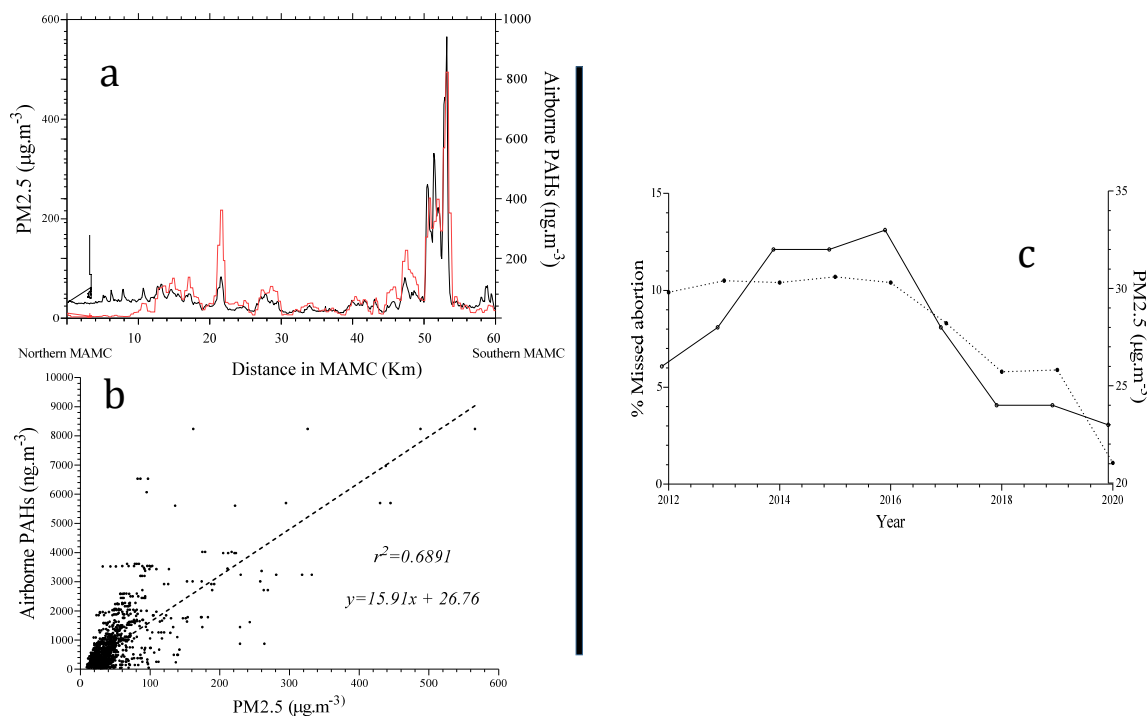


Figure 8. Analysis of tendency of PM2.5 in recent years in the MAMC vs. % missed abortion in women (24–34 years old). (a) Comparative series between PM2.5 and PAHs in MAMC (black line PM2.5 and redline total PAHs). (b) Correlation between airborne PAHs and PM2.5 (moderate correlation $r^2 = 0.69$). (c) Comparative series between missed abortion and PM2.5 in MAMC (dashed line % missed abortion and continuous line PM2.5).

It is well known that PAHs primarily stem from combustion sources that involve the incomplete pyrolysis of fossil fuels or, more generally, carbonaceous materials [27]. However, we found that vehicular combustion in the MAMC is the predominant source of PAHs in the air; this is supported by a significant correlation with primary combustion sources (see Figure 3). Additionally, lower levels of RET in the MAMC indicate that forest fires are not the principal source for PAH emissions, which emphasizes the relevance of vehicular contributions (see Figure 3). Therefore, PM2.5 exposure serves as a meaningful indicator of PAH exposure in the MAMC (Figure 8).

Expanding on these results, the annual series of missed abortion rates (2012–2020) in the MAMC showed a significant correlation with the annual average levels of PM2.5 (Pearson $r = 0.80$, $p < 0.01$) (see Figure 8c). Although this significant correlation does not imply causality, the analysis suggests an important connection between both variables. For instance, the critical year of 2016, which is marked by heightened air pollution in the MAMC, coincides with the highest missed abortion rate. In 2016, the average PM2.5 concentration exceeded $33 \mu\text{g} \times \text{m}^{-3}$, corresponding to a missed abortion rate of 10.3% (for ages ranging between 25 and 34 years old). Briefly, 2016 serves as an inflection point for both variables: prior to 2016, the PM2.5 levels were directly proportional to the missed abortion rate (uptrend), while after 2016, both series decreased (downtrend) (see Figure 8c).

Locally, within the MAMC, we found a preliminary association between PM2.5 (associated with PAHs) and the missed abortion rate. The MAMC has shown a missed abortion

rate of around 10% (2005–2016) among healthy women without comorbidities, aged between 25 and 34 years. Spatially, the missed abortion rate showed clear differences between the southern and the northern MAMC. The total PAH concentration in the southern region was 3.2 times higher than in the northern region; this is mainly attributed to industrial activities and vehicular traffic (see Figure 2).

4. Discussion

Given that the MAMC is located in the tropics (around 6.2 N), the diurnal temperature range exhibits more variability than the annual range and thus impacts the diurnal patterns of PAHs [28]. Specifically, the higher morning peak of PAHs may be attributed to the complex interactions between the surface temperature (night/early-morning gradient), thermal inversion, and condensation, which influence the dynamic of the gases and particles in the boundary layer. Additionally, a stable layer formed by condensed air particles in the early morning is resuspended due to temperature changes in the MAMC [29]. Also, the prevailing trade winds transport PM2.5 from the north to the south, potentially carrying PAHs from industrial/traffic sources along the predominant north–south wind pathway. Therefore, the levels of PAHs identified in the MAMC may represent a risk due to long-term exposure. The southern MAMC probably poses a higher risk for short-term exposure during pregnancy (see Figure 7). Figure 9 shows a suggested conceptual model for aerosol transport in the MAMC at a diurnal timescale which is consistent with the diurnal levels of PM2.5 reported in Sistema de Alertas Tempranas del Valle del Aburrá (SIATA—<https://siata.gov.co> accessed on 20 March 2020). This conceptual model also helps to explain why heavy congeners for PAHs, such as BaP, DahA, and IND, were predominantly found in the southern MAMC. Overall, higher PM2.5 levels are found in the southern MAMC between 23:00 and 7:00 am compared to the northern MAMC when the stable layer forms. The wind analysis reveals that despite some of the industries and the high number of vehicles per citizen found in the northern MAMC, the prevailing trade winds have an influence over the MAMC, moving from the north to the south of the valley and contributing to the transport of PM [30,31].

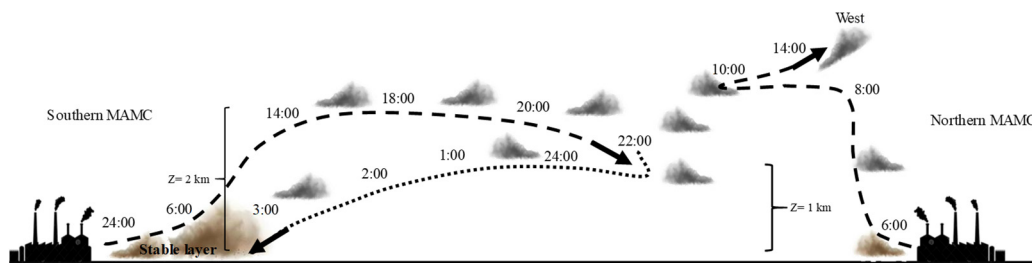


Figure 9. Conceptual model for diurnal cycle of wind direction–temperature and their effect on boundary layer height and aerosols transport in MAMC. The dotted lines show the aerosols transport.

At a global scale, the PM2.5 and the airborne PAHs have been linked with an increasing of the missed abortion rate [27]. Our previous study found that a mixture of PAH congeners associated with PM2.5 in the MAMC (see Figure 3), such as ANT, FLU, PYR, and BaP at low levels, may affect gestational hormone production, such as progesterone and β -hCG in a placental cell line, potentially explaining placental dysfunction and adverse pregnancy outcomes [32]. Certain PAHs associated with PM2.5, such as BaP, PYR, FLU, and ANT, were shown to induce hormone disorders in a placental cell line in that previous study [32]. While this is a cellular model, similar pathways linking miscarriage to air pollution exposure have been reported [33]. Furthermore, we previously evaluated the toxicity of PM in the MAMC, and the results indicated that PM decreased cell viability and induced reactive oxygen species (ROS) production. Both effects trigger DNA damage and the production of inflammatory mediators and are also involved in neurological diseases and even newborn-related issues [34]. For this reason, public health strategies in the MAMC should focus on the suitable management of PM2.5, an important source of particle-bound PAH emissions.

Implementing basic protective measures such as air masks has proven effective in reducing reproductive disorders during air pollution events.

Additionally, the I_a in the southern MAMC was shown to be higher than that in the northern region. In our cross-sectional study, the missed abortion rate in the south was 1.5 times higher than in the north; therefore, our results suggest a potential association between airborne PAHs and missed abortion in the MAMC. The exclusively residential areas (RES) located 50 m from vehicle and industrial emission sources showed lower exposure to PAHs by pregnant women. Additionally, we found higher concentrations of total PAHs in residential places with traffic and industrial influences, indicating that sources such as vehicles and industries in proximity to pregnant populations may elevate the risk of adverse perinatal outcomes. Nevertheless, it is crucial to note that this study is preliminary, and more extensive research should be conducted in the future to validate and expand upon these findings and to establish safety perimeters.

Human mobility was identified as a potential bias in this research, as pregnant women's exposure to PAHs might be influenced by mobility across various places. However, the primary exposure likely occurs in their residential places where they spend most of their time. Those limitations introduce uncertainties that should be dealt with in future studies. To overcome these challenges, advanced techniques such as remote sensors and geospatial big data analysis should be employed to accurately assess mobility patterns [35]. Finally, older individuals, pregnant women, and children should be considered as vulnerable populations during air pollution emergencies in the MAMC. In particular, safety perimeters in cities should be considered to prevent adverse pregnancy outcomes [36]. The missed abortion rate has been not deeply studied in the MAMC, and future research should include comorbidities as an additional study variable.

5. Conclusions

In this study, we conducted comprehensive air quality assessments in the Metropolitan Area of Medellin-Colombia, examining the levels, sources, and health implications of airborne polycyclic aromatic hydrocarbons (PAHs), with a particular focus on their association with PM2.5 and the potential impact on pregnancy outcomes.

Airborne PAH exposure in the MAMC was assessed using inhalation intake modelling (IIM) to identify receptor places for the risk assessment for pregnant women residing in the region. Also, through a cross-sectional application in the last 15 years, the missed abortion rate series were correlated with the average levels of PM2.5. This longitudinal analysis allowed us to discern potential associations between air quality and perinatal outcomes. Finally, by contrasting northern and southern regions of the MAMC, the PAH levels were compared with the missed abortion rate to identify the role played by the predominant direction of low-level atmospheric winds within the narrow valley where the MAMC is located. Despite the southern MAMC exhibiting a better employment rate, access to the health system, and per capita incomes, it unexpectedly reports a higher missed abortion rate than the northern MAMC. This fact suggests a potential association of missed abortion in the southern MAMC with the increased industrial and vehicular emissions, which are possibly exacerbated by the influence of trade winds.

The southern PAH levels are higher than those in the northern MAMC and coincide with a significant correlation between PM2.5 and missed abortion rates. As traffic and industrial activities are identified as the primary sources of PAHs in the MAMC, we suggest establishing safety perimeters for pregnancy development and ensuring that they are located far away from emission sources. Our findings highlight petrol emissions as the primary contributor to airborne PAHs, suggesting that transitioning to alternative fuels should be considered because the narrow morphology and thermal inversion in this valley decreases the atmospheric depuration. However, the industrial emissions should be controlled by the environmental authorities; the location of industries in the northern MAMC should also be evaluated, as dominant trade winds transport pollutants from the north to the south, influencing air quality. The highest risk was found in the southern

MAMC, implying that more intensive protection measures are required there. This higher risk may be related to the industrial and traffic sources influenced by air pollution dynamics in the MAMC.

Author Contributions: Conceptualization, F.J.M.-P.; methodology, S.V.A.-B., V.C.-G. and J.J.G.-L.; validation, C.D.R.-C., G.B.V.-G. and G.G.P.-C.; formal analysis, writing—original draft preparation and supervision, J.F.N.-V. and J.M.B.-S. All authors have read and agreed to the published version of the manuscript.

Funding: The materials and methods were supported by grants from Corporación Universitaria Remington (Project code: 4000000098 and project code 4000000316).

Institutional Review Board Statement: Not applicable.

Informed Consent Statement: Not applicable.

Data Availability Statement: Data are contained within the article.

Acknowledgments: The authors are thankful for the research project *Ensayo de disruptión endocrina de micro-contaminantes acumulados en prótesis mamarias de silicona por medio de passive dosing y expresión de la hormona β-hCG en la línea celular BeWo* (Project code: 4000000098). Furthermore, the authors are thankful for the research project *Escalamiento en procesos hidrológicos en los Andes de Colombia* (Project code: 4000000316). Finally, the authors thank the GAIA group for analyzing samples and for technical support.

Conflicts of Interest: The authors declare that there is no conflict of interest regarding the published results.

References

1. Phairuang, W.; Suwattiga, P.; Chetiyankornkul, T.; Hongtieab, S.; Limpaseni, W.; Ikemori, F.; Hata, M.; Furuuchi, M. The influence of the open burning of agricultural biomass and forest fires in Thailand on the carbonaceous components in size-fractionated particles. *Environ. Pollut.* **2019**, *247*, 238–247. [[CrossRef](#)] [[PubMed](#)]
2. Bo, M.; Salizzoni, P.; Clerico, M.; Buccolieri, R. Assessment of Indoor-Outdoor Particulate Matter Air Pollution: A Review. *Atmosphere* **2017**, *8*, 136. [[CrossRef](#)]
3. Kim, K.-H.; Jahan, S.A.; Kabir, E.; Brown, R.J.C. A review of airborne polycyclic aromatic hydrocarbons (PAHs) and their human health effects. *Environ. Int.* **2013**, *60*, 71–80. [[CrossRef](#)] [[PubMed](#)]
4. Green, R.S.; Malig, B.; Windham, G.C.; Fenster, L.; Ostro, B.; Swan, S. Residential Exposure to Traffic and Spontaneous Abortion. *Environ. Health Perspect.* **2009**, *117*, 1939–1944. [[CrossRef](#)]
5. La Marca, L.; Gava, G. Air pollution effects in pregnancy. In *Clinical Handbook of Air Pollution-Related Diseases*; Springer International Publishing: Cham, Switzerland, 2018; pp. 479–494. [[CrossRef](#)]
6. Korten, I.; Ramsey, K.; Latzin, P. Air pollution during pregnancy and lung development in the child. *Paediatr. Respir. Rev.* **2017**, *21*, 38–46. [[CrossRef](#)]
7. Dong, X.; Wang, Q.; Peng, J.; Wu, M.; Pan, B.; Xing, B. Transfer of polycyclic aromatic hydrocarbons from mother to fetus in relation to pregnancy complications. *Sci. Total Environ.* **2018**, *636*, 61–68. [[CrossRef](#)]
8. Yu, Y.; Wang, X.; Wang, B.; Tao, S.; Liu, W.; Wang, X.; Cao, J.; Li, B.; Lu, X.; Wong, M.H. Polycyclic Aromatic Hydrocarbon Residues in Human Milk, Placenta, and Umbilical Cord Blood in Beijing, China. *Environ. Sci. Technol.* **2011**, *45*, 10235–10242. [[CrossRef](#)]
9. Drwal, E.; Rak, A.; Gregoraszczuk, E.L. Review: Polycyclic aromatic hydrocarbons (PAHs)—Action on placental function and health risks in future life of newborns. *Toxicology* **2019**, *411*, 133–142. [[CrossRef](#)]
10. Detmar, J.; Rennie, M.Y.; Whiteley, K.J.; Qu, D.; Taniuchi, Y.; Shang, X.; Casper, R.F.; Adamson, S.L.; Sled, J.G.; Jurisicova, A.; et al. Fetal growth restriction triggered by polycyclic aromatic hydrocarbons is associated with altered placental vasculature and AhR-dependent changes in cell death. *Am. J. Physiol. Endocrinol. Metab.* **2008**, *295*, E519–E530. [[CrossRef](#)]
11. Perera, F.P.; Jedrychowski, W.; Rauh, V.; Whyatt, R.M. Molecular epidemiologic research on the effects of environmental pollutants on the fetus. *Environ. Health Perspect.* **1999**, *107* (Suppl. 3), 451–460. [[CrossRef](#)]
12. Naumova, Y.Y.; Eisenreich, S.J.; Turpin, B.J.; Weisel, C.P.; Morandi, M.T.; Colome, S.D.; Totten, L.A.; Stock, T.H.; Winer, A.M.; Alimokhtari, S.; et al. Polycyclic Aromatic Hydrocarbons in the Indoor and Outdoor Air of Three Cities in the U.S. *Environ. Sci. Technol.* **2002**, *36*, 2552–2559. [[CrossRef](#)] [[PubMed](#)]
13. Agarwal, P.; Singh, L.; Anand, M.; Taneja, A. Association Between Placental Polycyclic Aromatic Hydrocarbons (PAHS), Oxidative Stress, and Preterm Delivery: A Case–Control Study. *Arch. Environ. Contam. Toxicol.* **2017**, *74*, 218–227. [[CrossRef](#)] [[PubMed](#)]
14. Dai, Y.; Xu, X.; Huo, X.; Faas, M.M. Effects of polycyclic aromatic hydrocarbons (PAHs) on pregnancy, placenta, and placental trophoblasts. *Ecotoxicol. Environ. Saf.* **2023**, *262*, 115314. [[CrossRef](#)]

15. Nguyen, B.T.; Chang, E.J.; Bendikson, K.A. Advanced paternal age and the risk of spontaneous abortion: An analysis of the combined 2011–2013 and 2013–2015 National Survey of Family Growth. *Am. J. Obstet. Gynecol.* **2019**, *221*, 476.e1–476.e7. [\[CrossRef\]](#) [\[PubMed\]](#)

16. Bedoya-Soto, J.M.; Aristizábal, E.; Carmona, A.M.; Poveda, G. Seasonal Shift of the Diurnal Cycle of Rainfall Over Medellin’s Valley, Central Andes of Colombia (1998–2005). *Front. Earth Sci.* **2019**, *7*, 92. [\[CrossRef\]](#)

17. Poveda, G. La hidroclimatología de Colombia: Una síntesis desde la escala inter-decadal hasta la escala diurna. *Rev. Acad. Colomb. Cienc.* **2004**, *28*, 201–221. [\[CrossRef\]](#)

18. Rodriguez-Villamizar, L.A.; Rojas-Roa, N.Y.; Fernández-Niño, J.A. Short-term joint effects of ambient air pollutants on emergency department visits for respiratory and circulatory diseases in Colombia, 2011–2014. *Environ. Pollut.* **2019**, *248*, 380–387. [\[CrossRef\]](#)

19. Contreras, I.R.; Contreras, C.R.; Perez, F.M.; Grana, E.C. Optimization of an environmentally sustainable analytical methodology for the determination of polycyclic aromatic hydrocarbons in PM10 particulate matter. In Proceedings of the Conference Proceedings—Congreso Colombiano y Conferencia Internacional de Calidad de Aire y Salud Pública, CASAP 2019, Barranquilla, Colombia, 14–16 August 2019; Institute of Electrical and Electronics Engineers Inc.: Piscataway, NJ, USA, 2019. [\[CrossRef\]](#)

20. Tobiszewski, M.; Namieśnik, J. PAH diagnostic ratios for the identification of pollution emission sources. *Environ. Pollut.* **2012**, *162*, 110–119. [\[CrossRef\]](#)

21. Aral, M.M. *Environmental Modeling and Health Risk Analysis (Acts/Risk)*; Springer Science & Business Media: Dordrecht, The Netherlands, 2010.

22. Gil Ramírez, D.; Valderrama, J.F.N.; Tobón, C.A.P.; García, J.J.; Echeverri, J.D.; Sobotka, J.; Vrana, B. Occurrence, sources, and spatial variation of POPs in a mountainous tropical drinking water supply basin by passive sampling. *Environ. Pollut.* **2023**, *318*, 120904. [\[CrossRef\]](#)

23. Bedoya, J.; Martínez, E. Calidad del aire en el valle de aburrá Antioquia-Colombia. *DYNA* **2009**, *76*, 7–15.

24. Lung, S.-C.C.; Liu, C.-H. Fast analysis of 29 polycyclic aromatic hydrocarbons (PAHs) and nitro-PAHs with ultra-high performance liquid chromatography-atmospheric pressure photoionization-tandem mass spectrometry. *Sci. Rep.* **2015**, *5*, 12992. [\[CrossRef\]](#) [\[PubMed\]](#)

25. Šrám, R.J.; Binková, B.; Rössner, P.; Rubeš, J.; Topinka, J.; Dejmek, J. Adverse reproductive outcomes from exposure to environmental mutagens. *Mutat. Res./Fundam. Mol. Mech. Mutagen. Mutat.* **1999**, *428*, 203–215. [\[CrossRef\]](#) [\[PubMed\]](#)

26. Akhbarizadeh, R.; Dobaradaran, S.; Torkmahalleh, M.A.; Saeedi, R.; Aibaghi, R.; Ghasemi, F.F. Suspended fine particulate matter (PM2.5), microplastics (MPs), and polycyclic aromatic hydrocarbons (PAHs) in air: Their possible relationships and health implications. *Environ. Res.* **2021**, *192*, 110339. [\[CrossRef\]](#) [\[PubMed\]](#)

27. Zhu, X.; Fan, Z.; Wu, X.; Jung, K.H.; Ohman-Strickland, P.; Bonanno, L.J.; Lioy, P.J. Ambient concentrations and personal exposure to polycyclic aromatic hydrocarbons (PAH) in an urban community with mixed sources of air pollution. *J. Expo. Sci. Environ. Epidemiol.* **2011**, *21*, 437–449. [\[CrossRef\]](#) [\[PubMed\]](#)

28. Zhu, Y.; Yang, L.; Meng, C.; Yuan, Q.; Yan, C.; Dong, C.; Sui, X.; Yao, L.; Yang, F.; Lu, Y.; et al. Indoor/outdoor relationships and diurnal/nocturnal variations in water-soluble ion and PAH concentrations in the atmospheric PM2.5 of a business office area in Jinan, a heavily polluted city in China. *Atmos. Res.* **2015**, *153*, 276–285. [\[CrossRef\]](#)

29. Rendón, A.M.; Salazar, J.F.; Palacio, C.A.; Wirth, V.; Brötz, B. Effects of Urbanization on the Temperature Inversion Breakup in a Mountain Valley with Implications for Air Quality. *J. Appl. Meteorol. Clim.* **2014**, *53*, 840–858. [\[CrossRef\]](#)

30. Herrera-Mejía, L.; Hoyos, C.D. Characterization of the atmospheric boundary layer in a narrow tropical valley using remote-sensing and radiosonde observations and the WRF model: The Aburrá Valley case-study. *Q. J. R. Meteorol. Soc.* **2019**, *145*, 2641–2665. [\[CrossRef\]](#)

31. Correa, M.; Zuluaga, C.; Palacio, C.; Pérez, J.; Jiménez, J. Antioquia, Colombia surface wind coupling from free atmosphere winds to local winds in a tropical region within complex terrain. Case of study: Aburrá Valley Antioquia, Colombia. *Dyna* **2009**, *76*, 17–27.

32. Valderrama, J.F.N.; Gil, V.C.; Alzate, V.; Tavera, E.A.; Noreña, E.; Porras, J.; Quintana-Castillo, J.C.; García L, J.J.; Molina P, F.J.; Ramos-Contreras, C.; et al. Effects of polycyclic aromatic hydrocarbons on gestational hormone production in a placental cell line: Application of passive dosing to in vitro tests. *Ecotoxicol. Environ. Saf.* **2022**, *245*, 114090. [\[CrossRef\]](#)

33. Jing, G.; Yao, J.; Dang, Y.; Liang, W.; Xie, L.; Chen, J.; Li, Z. The role of β -HCG and VEGF-MEK/ERK signaling pathway in villi angiogenesis in patients with missed abortion. *Placenta* **2021**, *103*, 16–23. [\[CrossRef\]](#)

34. Marin-Palma, D.; González, J.D.; Narváez, J.F.; Porras, J.; Taborda, N.A.; Hernandez, J.C. Physicochemical Characterization and Evaluation of the Cytotoxic Effect of Particulate Matter (PM10). *Water Air Soil Pollut.* **2023**, *234*, 138. [\[CrossRef\]](#)

35. Song, Y.; Huang, B.; He, Q.; Chen, B.; Wei, J.; Mahmood, R. Dynamic assessment of PM2.5 exposure and health risk using remote sensing and geo-spatial big data. *Environ. Pollut.* **2019**, *253*, 288–296. [\[CrossRef\]](#) [\[PubMed\]](#)

36. Zhu, W.; Zheng, H.; Liu, J.; Cai, J.; Wang, G.; Li, Y.; Shen, H.; Yang, J.; Wang, X.; Wu, J.; et al. The correlation between chronic exposure to particulate matter and spontaneous abortion: A meta-analysis. *Chemosphere* **2022**, *286*, 131802. [\[CrossRef\]](#) [\[PubMed\]](#)